

1
2
3
4
5
6
7
8
9
10
11
12
13
14
15
16
17
18
19
20
21
22
23
24
25
26
27
28
29

Aging alters envelope representations of speech-like sounds in the inferior colliculus

Aravindakshan Parthasarathy^{1,2,#}, Björn Herrmann^{3,#}, Edward L. Bartlett^{1*}

¹ Depts. of Biological Sciences and Biomedical Engineering, Purdue University,
West Lafayette, IN, 47906, USA

² Dept. of Otolaryngology, Harvard Medical School, and Eaton-Peabody Laboratories,
Massachusetts Eye and Ear Infirmary, Boston, MA 02114

³ Department of Psychology & Brain and Mind Institute, The University of Western Ontario,
London, ON, N6A 3K7, Canada

#Aravindakshan Parthasarathy and Björn Herrmann contributed equally to this work.

*Correspondence concerning this article should be addressed to Edward L Bartlett, 206 S. Martin
Jischke Drive, West Lafayette, IN - 47906. E-mail: ebartle@purdue.edu

Running title: Envelope coding deficits with age in the IC

Number of pages: 31

Number of figures: 6

Number of words:

Abstract: 228

Introduction: 626

Discussion: 1438

Conflict of Interest: The authors declare no competing conflicts of interest

30 **ABSTRACT**

31 Older listeners often experience difficulties understanding speech in the presence of background
32 sound. These deficits are thought to reflect neural deficits in the central auditory pathway, as they
33 can occur independent of changes in cochlear hearing thresholds. Here we used a systems-level
34 (scalp recordings) and a microcircuit-level (extracellular recordings) approach in male Fischer-344 rats
35 to investigate how aging affects sensitivity to the temporal envelopes of speech-like sounds in the
36 inferior colliculus. Scalp-recorded potentials suggest an age-related increase in sensitivity to
37 temporal regularity along the ascending auditory pathway. The underlying cellular changes in the
38 midbrain were examined using extracellular recordings from inferior colliculus neurons. We used the
39 local field potential (LFP) as a proxy for a neuron's or neural population's synaptic inputs, and unit
40 activity as a measure of spiking output. We observed an age-related increase in sensitivity to the
41 sound's onset and temporal regularity (i.e., periodicity envelope) in the spiking output of inferior
42 colliculus neurons, relative to their synaptic inputs. This relative enhancement for aged animals was
43 most prominent for multi-unit (in contrast to single-unit) spiking activity. Spontaneous multi-unit,
44 but not single-unit, activity was also enhanced in aged compared to young animals. Our results
45 suggest that aging is associated with altered sensitivity to sound and a sound's temporal regularities,
46 and that these effects may be due to increased gain of neural network activity in the aged auditory
47 midbrain.

48
49 **SIGNIFICANCE STATEMENT**

50 Older listeners commonly experience challenges understanding speech in the presence of
51 background sound. The neural functional changes contributing to this problem remain unclear. Our
52 study shows an increase in network-level neuronal activity in the auditory midbrain of aged animals
53 that alters the sensitivity to temporal regularities in speech sounds. Sensitivity is abnormally
54 heightened despite reduced synaptic input to neurons, which suggest aberrant gain control
55 mechanisms that are associated with aging. Although an increased gain in the auditory pathway of
56 aged listeners may support detection of temporal regularities in speech, it may come at the cost of
57 reduced discrimination between multiple speakers, and thus may contribute to age-related
58 difficulties in understanding speech.

59

60 **Keywords:** inferior colliculus, voice onset time, evoked potentials, hearing loss

61

Introduction

62 Older and middle-aged listeners experience difficulties understanding speech, particularly in
63 challenging listening situations such as in the presence of background sounds, competing speakers,
64 or reverberation (Ruggles et al., 2011, Pichora-Fuller and Souza, 2001). Speech perception depends
65 on the sensitivity of the auditory system to temporal regularities in sounds. Temporal regularities in
66 speech may be divided into three categories: the slow fluctuations (<50 Hz) of the speech envelope
67 that capture word and syllabic rate; the periodicity envelope (50–500 Hz), which contains the
68 fundamental frequency of the speaker’s voice (f_0) and is crucial for speaker identification (Bregman,
69 1990); and the temporal fine structure (>500 Hz), which contains information about formant structure
70 (Rosen, 1992). The sensitivity of the auditory system to temporal regularity in sounds declines with
71 age, with drastic consequences for speech perception (Walton, 2010, Fullgrabe et al., 2015, Anderson
72 et al., 2011), but the neurophysiological changes that underlie this age-related decline are not well
73 understood.

74 An age-related decline in temporal processing abilities with age is thought to be primarily neural
75 in origin, because it is independent of changes in hearing thresholds due to impaired cochlear
76 function (Frisina and Frisina, 1997, Pichora-Fuller and Souza, 2001, Gordon-Salant and Fitzgibbons,
77 2001). The neural deficits that may contribute to impaired sensitivity to temporal regularity include
78 cochlear synaptopathy – that is, the degradation of cochlear synapses between inner hair cells and
79 auditory nerve fibers (Sergeyenko et al., 2013) – and a decrease in inhibitory neurotransmitters in the
80 brainstem, midbrain and cortex (Caspary et al., 2008, Takesian et. al., 2009, Rabang et al., 2012). Loss of
81 inhibition may result in increased neural activity in central auditory regions despite diminished inputs
82 from peripheral structures (Mohrle et al., 2016, Parthasarathy et al., 2014, Hughes et al., 2010).

83 However, it is less clear how aging affects sensitivity to temporal regularity in central auditory regions,
84 in particular for complex, speech-like sounds.

85 Previous work suggests that neurons in the inferior colliculus show altered temporal processing
86 including changes in the sensitivity to the temporal regularities in sounds (Walton et al., 2002, Walton
87 et al., 1998, Palombi et al., 2001, Rabang et al., 2012, Schatterman et al., 2008). These studies focused
88 on neuronal spiking, which reflects the output of neurons. In contrast, local field potentials (LFPs) are
89 thought to mostly reflect the summed synaptic inputs to a neuron or local neuronal population
90 (Buzsaki et al., 2012, Logothetis and Wandell, 2004, Logothetis et al., 2001). Recent recordings of LFPs
91 and spiking activity show that synchronization of spiking activity (output) is abnormally enhanced in
92 the aging inferior colliculus, despite decreased synaptic inputs (input), and that this age-related
93 relative increase in activity (i.e., from a neuron's input to its output) is specific for sounds with
94 modulation rates below 100 Hz (Herrmann et al., 2017). Whether aging also leads to an over-
95 sensitivity to temporal regularities in complex, speech-like sounds is unknown.

96 In the current study, we test the hypothesis that neural synchronization to the periodicity
97 envelope (~100 Hz) of speech is abnormally enhanced in the inferior colliculus of aged animals. We
98 assess peripheral neural function by measuring wave 1 amplitudes of the auditory brainstem
99 responses (ABRs) and show physiological evidence for cochlear synaptopathy in aged animals. Scalp-
100 recorded neural synchronization to the envelope of a speech-like stimulus is increased specifically in
101 more rostral regions in the auditory pathway compared to more caudal ones. Further, we assess the
102 relation between LFPs (synaptic input) and spiking output in the inferior colliculus using extracellular
103 recordings. Synchronization of synaptic activity to the envelope of a speech-like sound is decreased
104 in aged animals, whereas synchronization of spiking activity from well isolated units does not differ

Envelope coding deficits with age in the IC

5

105 between age groups. Multi-unit spike synchronization, however, is drastically increased for aged
106 animals, suggesting changes in gain control mechanisms occurring largely at a neural network level.

107 **Methods and Materials**

108 ***Ethical approval***

109 The experimental procedures described in the present investigation were approved by the
110 Institutional Animal Care and Use Committee of Purdue University (PACUC #1111000167). The
111 experiments included in this study comply with the policies and regulations described by
112 (Drummond, 2009). Rats were housed one per cage in accredited facilities (Association for the
113 Assessment and Accreditation of Laboratory Animal Care) with food and water provided *ad libitum*.
114 The number of animals used was reduced to the minimum necessary to allow adequate statistical
115 analyses.

116 ***Experimental Design and Statistical analysis***

117 The study design is cross-sectional. The number of animals used per group along with details of the
118 critical variables and statistical tests for each specific analysis can be found in the subsections devoted
119 to each analysis. In short, 11 young (3–6 months, ~300 g) and 12 aged (22–26 months, ~400–500 g)
120 male Fischer-344 rats were used for scalp recordings and 11 young (3–6 months, ~300 g) and 9 aged
121 (22–26 months, ~400–500 g) male Fischer-344 rats were used for extracellular recordings. Age group
122 differences were tested Wilcoxon's rank sum test (using the ranksum function in Matlab; Mathworks,
123 USA). Throughout the manuscript, effect sizes are provided as r_e ($r_{\text{equivalent}}$; Rosenthal and Rubin, 2003).
124 r_e is equivalent to a Pearson product-moment correlation for two continuous variables, to a point-

125 biserial correlation for one continuous and one dichotomous variable, and to the square root of
126 partial η^2 for an analysis of variance.

127 ***Stimulus generation***

128 Sound stimuli were generated using SigGenRP (Tucker-Davis Technologies, TDT) at a 97.64 kHz
129 sampling rate (standard TDT sampling rate) and presented through custom-written interfaces in
130 OpenEx software (TDT). Sound waveforms were generated via a multichannel processor (RX6, TDT),
131 amplified (SA1, TDT), and presented free-field through a Bowers and Wilkins DM601 speaker. The
132 output from the speaker was calibrated free field, using SigCal (TDT) and a Bruel Kjaer microphone
133 with a 0.25-in. condenser, pointed at frontal incidence to the speaker, from the same location as the
134 animal's right ear, and was found to be within ± 6 dB for the frequency range tested. All recordings
135 took place in an Industrial Acoustics booth lined with 1 inch (35 mm) Sonex foam with ~90%
136 absorption for frequencies ≥ 1000 Hz, minimizing potential echoes or reverberations. All analyses
137 described below accounted for the travel time of the sound wave from the speaker to the animals'
138 ears.

139 ***Sound stimulation***

140 The stimulus was a natural English syllable, /ba/, which was 260ms long and spoken by a male speaker
141 of North American English with a fundamental frequency ~ 110 Hz. In order to account for the
142 differences in the hearing range between rats and humans, as well as to increase the number of
143 responsive neurons in the inferior colliculus of rats, this speech token was half-wave rectified, and
144 used to modulate a broadband noise carrier (0.04–40 kHz) (Figure 1A). This preserved the periodicity
145 envelope as well as the original fine structure of the speech token, both of which served as the
146 modulator for the broadband noise (Figure 1B, C).

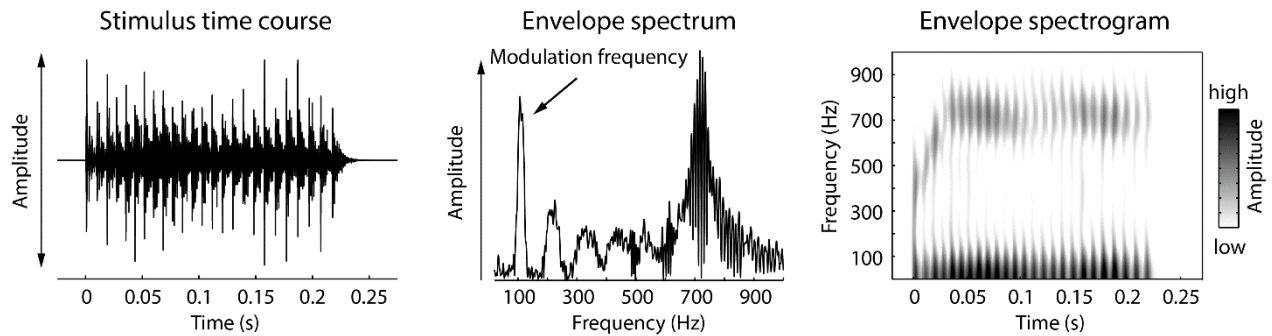


Figure 1: Speech-like sound used in the current study. Left: Waveform of the speech-like sound. **Middle:** Amplitude spectrum of the envelope of the speech-like sound displayed on the left. **Right:** Spectrogram of the envelope of the speech-like sound.

147 ***Electrophysiological recordings at the scalp***

148 11 young (3–6 months, ~300 g) and 12 aged (22–26 months, ~400–500 g) male Fischer-344 rats
149 obtained from Charles River Laboratories were used for the scalp recordings. The aging Fisher-344 rat
150 has been suggested to be a suitable model to study presbycusis in aging animals (Syka, 2010) and
151 has been shown to exhibit high frequency hearing loss and metabolic presbycusis that are
152 characteristic of human age-related loss of hearing sensitivity (Dubno et al., 2013, Allen and Eddins,
153 2010).

154 Methods for experimental setup, sound stimulation, and scalp-potential recordings are similar
155 to those described before (Parthasarathy et al., 2016, Parthasarathy et al., 2014). The animals were
156 briefly anesthetized using isoflurane (1.5–2%) for the insertion of subdermal needle electrodes
157 (Ambu) and the intramuscular injection of dexmedetomidine (Dexdomitor, 0.2 mg/kg), an α -
158 adrenergic agonist that acts as a sedative and an analgesic. Recordings commenced after a 15 minute
159 recovery from the anesthesia, and were terminated if the animal showed any signs of discomfort as
160 monitored by a video camera in the recording chamber.

161 The scalp-evoked responses to the temporal envelope of the speech-like sound (Envelope
162 following response - EFR) were obtained using two simultaneous recording channels. One positive

163 electrode (caudal channel) was placed on the animal's forehead along the midline at Cz – Fz. This
164 electrode has a strong wave 3 ABR component (cochlear nuclei) and best sensitivity to modulation
165 frequencies ≥ 100 Hz (Parthasarathy and Bartlett 2012). Another positive electrode (rostral channel)
166 was placed horizontally, along the inter-aural line, above the location of the inferior colliculus. This
167 electrode has a strong wave 1, 4 and 5 ABR components (auditory nerve, the inferior colliculus and its
168 afferents) and best sensitivity to modulation frequencies < 100 Hz (Parthasarathy and Bartlett, 2012).
169 The negative electrode was placed under the right ear, along the mastoid, and the ground was placed
170 in the nape of the neck. Impedances were ensured to be always less than $1\text{K}\Omega$ as tested using the low-
171 impedance amplifier (RA4LI, Tucker Davis Technologies or TDT).

172 This two-channel setup allowed greater sensitivity to different ranges of modulation frequencies
173 and putative generators compared to recording from a single channel alone, as reported previously
174 (Parthasarathy and Bartlett, 2012). Signal presentation and acquisition were performed by BioSig
175 software (TDT). The stimulus was presented free field to the right of the animal, at a distance of 115 cm
176 from speaker to the right ear. Digitized waveforms were recorded with a multichannel recording and
177 stimulation system (RZ-5, TDT) and analyzed with BioSig or custom written programs in MATLAB
178 (Mathworks).

179 ***Surgical procedures for extracellular recordings***

180 11 young (3–6 months, ~300 g) and 9 aged (22–26 months, ~400–500 g) male Fischer-344 rats were
181 used for extracellular recordings. Methods for surgery, sound stimulation and recording are similar to
182 those described in (Herrmann et al., 2015, Rabang et al., 2012). Surgeries and recordings were
183 performed in a 9'x9' double walled acoustic chamber (Industrial Acoustics Corporation). Animals
184 were anesthetized using a mixture of ketamine (VetaKet, 80 mg/kg) and dexmedetomidine
185 (Dexdomitor, 0.2 mg/Kg) administered intra-muscularly via injection. A constant physiological body

186 temperature was maintained using a water-circulated heating pad (Gaymar) set at 37°C with the
187 pump placed outside the recording chamber to eliminate audio and electrical interferences. The
188 animals were maintained on oxygen through a manifold. The pulse rate and oxygen saturation were
189 monitored using a pulse-oximeter to ensure they were within normal ranges during surgery.
190 Supplementary doses of anesthesia (20mg/kg of ketamine, 0.05mg/kg of dexmedetomidine) were
191 administered intra-muscularly as required to maintain areflexia and a surgical plane of anesthesia. An
192 initial dose of dexamethasone and atropine was administered prior to incision to reduce swelling and
193 mucosal secretions. A subdermal injection of Lidocaine (0.5 ml) was administered at the site prior to
194 first incision. A central incision was made along the midline, and the calvaria exposed. A stainless steel
195 headpost was secured anterior to bregma using an adhesive and three screws drilled into the skull to
196 provide structural support for a head-cap, constructed of orthodontic resin (Dentsply). A craniotomy
197 was performed from 9–13 mm posterior to bregma, which extended posterior to the lambda suture,
198 and 3 mm wide extending from the midline. The dura mater was kept intact, and the site of recording
199 was estimated stereotaxically using a rat atlas (Paxinos and Watson, 2006) as well as using internal
200 vasculature landmarks and physiological measurements. At the completion of recordings, animals
201 were euthanized with Beuthanasia (200 mg/kg IP). Once areflexive, they were perfused transcardially
202 with 150–200 mL phosphate buffered saline with followed by 400–500 mL 4% paraformaldehyde. The
203 brain was then removed and stored or processed further for Nissl or immunohistochemistry.

204 ***Electrophysiological recordings in extracellular space***

205 Neural activity in inferior colliculus was recorded *in vivo* using a tungsten microelectrode (A-M
206 Systems) encased in a glass capillary that was advanced using a hydraulic micro-drive (Narishige). We
207 recorded 118 units in young rats and 121 units in aged rats. The inferior colliculus was identified based
208 on short-latency driven responses to tone stimuli. The central nucleus of the inferior colliculus was

209 identified using the ascending tonotopy moving in a dorsoventral direction as well as narrowly tuned
210 responses to pure tones with frequencies ranging from 0.5 to 40 kHz. Recordings were obtained from
211 both the dorsal cortex and central nucleus. Although we cannot exclude that we recorded from dorsal
212 and lateral (or external) cortex, based on the recording depth, the presence of sustained responses
213 to tones and amplitude-modulated stimuli, as well as clear frequency tuning in most cases, we
214 estimate that most of our units were recorded from the central nucleus.

215 The sounds were presented to the animal at azimuth 0° and elevation 0° . Neural signals were
216 acquired using the tungsten microelectrode connected to a headstage (RA4, TDT) and were amplified
217 (RA4PA preamplifier, TDT). The digitized waveforms and spike times were recorded with a
218 multichannel recording and stimulation system (RZ-5, TDT) at a sampling rate of 24.41 kHz (standard
219 TDT sampling rate). The interface for acquisition and spike sorting were custom made using the
220 OpenEx and RpvdsEx software (TDT). The units acquired were filtered between 500 Hz (occasionally
221 300 Hz) and 5000 Hz. The acquired spikes were stored in a data tank and analyzed using custom
222 written software in Matlab. Local field potentials were simultaneously recorded from the same
223 electrode by sampling at 1525.88 Hz and bandpass filtering from 3 to 500 Hz.

224 ***Assessment of peripheral and brainstem function***

225 Auditory brainstem responses (ABRs) were recorded using the scalp-recording setup described
226 above. ABRs were recorded in response to brief broadband click stimuli of 0.1-ms duration that varied
227 in sound levels from 5 to 95 dB SPL in 10 dB steps. The stimuli were presented in alternating polarity
228 at 26.6 clicks per second. The acquisition window was 20 ms, and each ABR was an average of 1,500
229 repetitions. The ABR amplitudes of different waves were calculated as the amplitude of the peak of
230 the wave from the baseline, in BioSig (TDT). ABRs between groups were compared at peak response
231 level, which was determined as the lowest sound level that produced the maximum amplitude for

232 each animal. This typically corresponded to 70–75 dB sound pressure level (SPL) for the young and
233 80–85 dB SPL for the aged rats.

234 ***Analysis of neural synchronization recorded at the scalp***

235 For scalp recorded neural synchronization (i.e., EFRs), the speech-like stimulus (described above) was
236 presented with a repetition rate of 3.1 Hz. The stimulus was presented at peak response level
237 described above, which was determined following a fast-Fourier transform (FFT) of the time-domain
238 response. Each response time course was obtained as an average of 200 stimulus repetitions in
239 alternating polarity. Responses were filtered online between 30–3000 Hz with a 60 Hz notch filter.

240 In order to analyze the fidelity of the auditory system to synchronize with the temporal structure
241 in the speech-like sound, we first used a broad-scale approach by calculating the correlation between
242 the stimulus waveform and the response time course for lags ranging from 0 to 0.05 s. This cross-
243 correlation approach was calculated twice, once for a low-frequency range (i.e., stimulus waveform
244 and response time course were low-pass filtered at 300 Hz; Butterworth) and once for a high-
245 frequency range (i.e., stimulus waveform and response time course were band-pass filtered from 300
246 to 3000 Hz; Butterworth). The former assessed neural synchronization to the vowel-like envelope
247 periodicity, the latter assessed neural synchronization to the temporal fine structure in the stimulus.
248 The highest correlation value (out of all lags) was used as a measure of synchronization strength.
249 Separately for the two channels and the two filtered signals, Wilcoxon's rank sum test (Matlab:
250 ranksum) was used to test whether correlation values differed between age groups.

251 We further investigated neural synchronization by calculating the amplitude spectrum (using a
252 fast Fourier transform [FFT]; Hann window; zero-padding) of the averaged time-domain signal. Neural
253 synchronization could not be quantified as inter-trial phase coherence (Lachaux et al., 1999) because
254 the recordings were averaged across trials online. This analysis focused on neural synchronization to

255 the envelope of the speech-like sound (~110 Hz) and we thus averaged the spectral amplitudes in
256 the frequency window ranging from 105–115 Hz. Wilcoxon's rank sum test (Matlab: ranksum) was
257 used to test whether neural synchronization to the envelope differed between age groups (separately
258 for the caudal and rostral channel).

259 ***Analysis of local field potentials (LFPs)***

260 Local field potentials were notch filtered at 60 Hz and 120 Hz (elliptic filter; infinite-impulse response
261 [IIR]; zero-phase lag) to suppress line noise, and low-pass filtered at 200 Hz (Butterworth; IIR; zero-
262 phase lag).

263 For the time-domain analysis, single-trial time courses were averaged separately for each age
264 group. Onset responses were analyzed by calculating the root-mean-square (RMS) amplitude of the
265 averaged signal in the 0–0.08 s time window. Wilcoxon's rank sum test (Matlab: ranksum) was used
266 to test differences in sound-onset responses between age groups.

267 Neural synchronization was analyzed by calculating a normalized vector strength spectrum
268 (Wolff et al., 2017, Herrmann et al., 2017). To this end, for each trial, a fast Fourier transform (FFT; Hann
269 window; zero-padding) was calculated using the data ranging from 0.08 s to 0.225 s post sound onset
270 (frequency range: 20–180 Hz; step size: 0.05 Hz; zero-padding). An inter-trial phase coherence (ITPC)
271 spectrum was calculated using the complex values from the FFT (Lachaux et al., 1999). An ITPC
272 permutation distribution was generated by flipping the sign of a random subset of trials (Wolff et al.,
273 2017), followed by ITPC calculation. This procedure was repeated 200 times and resulted in a
274 permutation distribution of ITPC values. The spectrum of normalized vector strength was calculated
275 by subtracting the mean ITPC of the permutation distribution from the empirically observed ITPC and
276 dividing the result by the standard deviation of the permutation distribution (separately for each

277 frequency). The normalized ITPC (vector strength) reflects a statistical measure – that is, a z-score –
278 with a meaningful zero that indicates non-synchronized activity.

279 In order to test for differences in neural synchronization at the envelope frequency between age
280 groups, the normalized vector strength was averaged across the 105–115 Hz frequencies. Wilcoxon’s
281 rank sum test (Matlab: ranksum) was used to test whether neural synchronization differed between
282 age groups.

283 ***Analysis of multi-unit activity (MUA)***

284 Multi-unit activity was extracted based on the recorded broad-band neural signal (Lakatos et al., 2013,
285 Lakatos et al., 2005). To this end, the signal was high-pass filtered at 300 Hz (Butterworth; IIR; zero-
286 phase lag), full-wave rectified by calculating absolute values, low-pass filtered at 200 Hz (Butterworth;
287 IIR; zero-phase lag), and down-sampled to the sampling frequency of the LFP (1525.88 Hz). Data
288 analysis followed closely the analysis of LFP data.

289 For the time-domain analysis, single-trial time courses were averaged separately for each age
290 group. Onset responses were analyzed by calculating the mean amplitude of the averaged signal in
291 the 0–0.08 s time window. Wilcoxon’s rank sum test (Matlab: ranksum) was used to test differences in
292 sound-onset responses between age groups.

293 Neural synchronization was analyzed by calculating a normalized vector strength spectrum
294 using the same procedure as described for the LFP data.

295 ***Analysis of single-unit activity (SUA)***

296 Overall, we recorded from 89 single units in young, and 123 single units in the aged animals. Single
297 unit activity was isolated online during the recordings of the neural signals. Units that were
298 substantially above noise threshold were sorted visually online, and then subsequently identified and

299 isolated based on waveform similarity offline, using the OpenEx interface. Isolated single units had
300 an SNR of at least 6 dB relative to the surrounding noise floor and stable waveform shapes. The
301 acquired spikes were stored in data tank and analyzed using custom-written software in MATLAB.

302 Peri-stimulus time histograms were calculated by convolving an impulse vector generated from
303 spike times with a Gaussian function with a standard deviation of 3 ms (Dayan and Abbott, 2001).
304 Neural responses to the onset of the sound was investigated by calculating the mean firing rate for
305 the 0–0.08 s time window. Wilcoxon’s rank sum test (Matlab: ranksum) was used to test differences in
306 sound-onset responses between age groups.

307 Investigation of neural synchronization was assessed using normalized vector strength based on
308 spike times (Herrmann et al., 2017). To this end, spike times (within the 0.08–0.225 s time window)
309 were transformed to phase angles (\mathbf{p}) using the following formula:

310
$$\mathbf{p} = 2 f \mathbf{t} \pi + \pi$$

311 , where f is frequency and \mathbf{t} a vector of spike times. Phase angles were wrapped to range from $-\pi$
312 to π . The empirical vector strength v (similar to ITPC described above), that is, the resultant vector
313 length, was calculated as follows (Lachaux *et al.*, 1999):

314
$$v = \frac{1}{n} \left| \sum_{j=1}^n e^{ip_j} \right|$$

315
316 , where v is the vector strength, i the imaginary unit, \mathbf{p} the vector of phase angles, and n the
317 number of spikes (with j being the index). Vector strength can be biased by the number of spikes,
318 with smaller v values for a higher number of spikes. In order to avoid biases estimates, a distribution
319 of random vector strength values was calculated. That is, n (number of spikes) random phase values
320 between $-\pi$ and π were generated and the vector strength (i.e., the resultant vector length) was

321 calculated. Randomly drawing phase values and calculation of the vector strength was repeated 1000
322 times, which resulted in a distribution of random vector strengths given the number of spikes. The
323 normalized vector strength was then calculated by subtracting the mean of the random vector
324 strength distribution from the empirical vector strength and dividing the result by the standard
325 deviation of the random vector strength distribution. The normalized vector strength was calculated
326 for frequencies (f) ranging from 20 Hz to 180 Hz with a frequency resolution of 0.1 Hz, resulting in a
327 vector strength spectrum. In order to test for differences in neural synchronization at the envelope
328 frequency between age groups, the normalized vector strength was averaged across the 105–115 Hz
329 frequencies. Wilcoxon's rank sum test was used to test whether neural synchronization differed
330 between age groups.

331

Results

332 ***ABR amplitudes are reduced in aged animals***

333 ABRs were recorded simultaneously from two electrode montages – one that emphasizes more
334 caudal generators (putatively including the auditory nerve and the cochlear nucleus), and another
335 that emphasizes more rostral generators (putatively including the inferior colliculus), as evidenced by
336 the differences in ABR waveform morphology, modulation rate sensitivity, and the effects of
337 anesthesia (Parthasarathy and Bartlett, 2012, Parthasarathy et al., 2014).

338 ABR wave 1 amplitudes were significantly decreased for aged compared to young rats (Figure
339 2A, rostral channel: $p = 1.96 \times 10^{-4}$, $r_e = 0.701$, $df = 21$; caudal channel: $p = 7.20 \times 10^{-5}$, $r_e = 0.732$, $df = 21$). The
340 wave 1 of the ABR originates in the auditory nerve, and its amplitude at suprathreshold sound levels
341 is a physiological indicator for the degree of cochlear synaptopathy due to aging or noise exposure

342 (Sergeyenko et al., 2013, Stamper and Johnson, 2015). This age-related decrease in ABR amplitudes
343 was also observed for all subsequent waves (wave 3: $p = 5.55 \times 10^{-5}$, $r_e = 0.739$, $df = 21$; wave 4: $p = 9.92 \times 10^{-4}$, $r_e = 0.641$, $df = 21$; wave 5: $p = 7.17 \times 10^{-5}$, $r_e = 0.732$, $df = 21$; Figure 2A) with generators in other
344 brainstem and midbrain nuclei. Hence, there was an overall reduction in transient responses in the
345 auditory nerve fibers, auditory brainstem and midbrain with age.
346

347 ***Scalp-recorded neural synchronization shows strong spectral peaks and stimulus correlation with***
348 ***age despite weak ABR amplitudes***

349 The ability of the auditory system to represent the various temporal regularities of speech were
350 assessed using a measure of neural synchronization (i.e., EFR) evoked to the speech-like sound. The
351 sensitivity of neural activity to the sound's temporal structure was assessed in two ways: Cross-
352 correlation and spectral amplitude (derived from a fast Fourier transform). The overall temporal
353 sensitivity was calculated by cross-correlating the time course of the scalp-recorded neural response
354 with the stimulus time course. In the caudal channel, cross-correlation values were reduced for aged
355 compared to young rats ($p = 1.54 \times 10^{-4}$, $r_e = 0.709$, $df = 21$) for the 300–3000-Hz frequency range that
356 contains information about the sound's temporal fine structure. There was no difference in
357 correlation values between young and aged animals for the <300-Hz frequency range (envelope) ($p = 0.479$, $r_e = 0.155$, $df = 21$; Figure 2B, left). In the rostral channel with putative generators in the
358 midbrain and its afferents, there was no age difference for the 300–3000-Hz frequency range ($p = 0.069$, $r_e = 0.385$, $df = 21$). However, aging was associated with an increase in correlation values for
359 the <300 Hz range (envelope) ($p = 0.034$, $r_e = 0.444$, $df = 21$; Figure 2B, right).
360
361

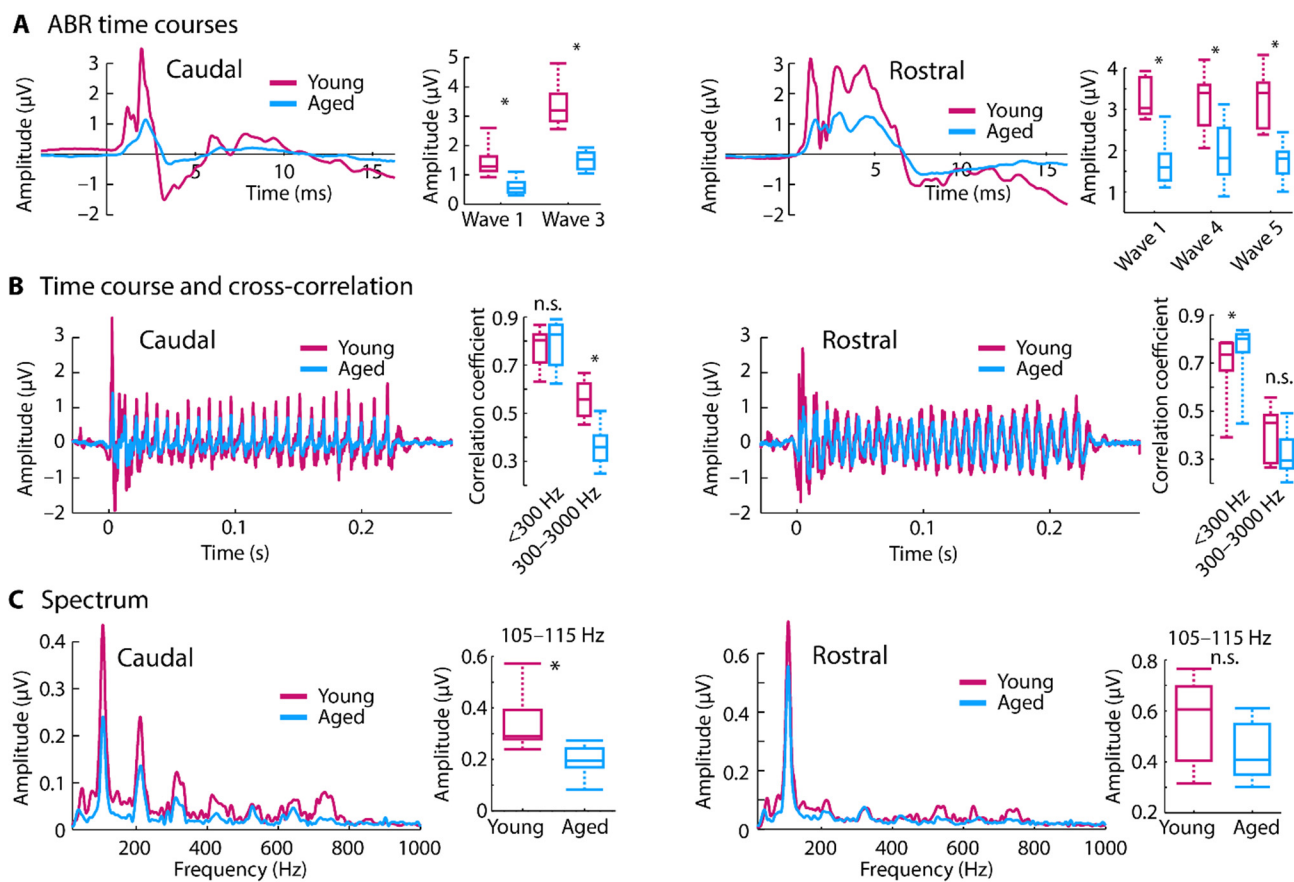


Figure 2: Scalp-recorded potentials simultaneously recorded in two channels emphasizing rostral versus caudal generators. A: Click-evoked auditory brainstem responses (ABRs) and amplitudes for different ABR waves. **B:** Time courses of envelope following responses (EFRs) in response to the speech-like /ba/ sound. Boxplots show coefficients from the cross-correlation for different frequency bands. **C:** Amplitude spectra derived from fast Fourier transforms. Boxplots show neural synchronization strength to the sound's F0 envelope (105–115 Hz). * $p < 0.05$, n.s. – not significant

362 Spectral amplitudes derived via a fast Fourier transform were averaged in the 105–115 Hz
 363 frequency band to assess neural synchronization to the temporal envelope (i.e., fundamental
 364 frequency; F0) of the speech-like sound. For the caudal channel, neural synchronization at the
 365 envelope frequency was larger for young compared to aged rats ($p = 1.96 \times 10^{-4}$, $r_e = 0.701$, $df = 21$; Figure
 366 2C, left). Although there was a similar trend in the rostral channel, this was not statistically significant
 367 ($p = 0.069$, $r_e = 0.385$, $df = 21$; Figure 2C, right).

368 Taken together, our neural synchronization measures show that for caudal generators (auditory
369 nerve, cochlear nucleus) synchronization was either similar or increased for younger compared to
370 aged rats, whereas for rostral generators (lateral lemniscus, inferior colliculus) synchronization was
371 either similar or increased for aged compared to younger rats. These data may suggest an age-related
372 relative increase in synchronization strength along the ascending auditory pathway. Extracellular
373 recordings from inferior colliculus neurons were obtained to further explore the age-related gain
374 increases in the auditory system to the complex, speech-like sound.

375 ***LFP onset response and neural synchronization to the envelope are reduced in aged animals***

376 Although changes in the neural representation of the speech-like sound were observed in the scalp-
377 recorded synchronization measures, these EFRs reflect the superposition of activity from multiple
378 generators. In order to localize age-related changes to the inferior colliculus and its afferents, we used
379 LFPs as a proxy for the synaptic input to the inferior colliculus neurons. LFP time courses are displayed
380 in Figure 3A. Neural responses to the sound onset (RMS amplitude 0–0.08 s) was larger for young
381 compared to aged animals ($p = 4.47 \times 10^{-9}$, $r_e = 0.368$, $df = 237$; Figure 3A right), suggesting that the
382 strength of the synaptic inputs to the inferior colliculus neurons decrease with age.

383 In order to investigate whether this decrease in synaptic input is accompanied by a decrease in
384 LFP synchronization, the normalized vector strength at the F0 frequency (105–115 Hz) was measured
385 in the sustained response of the LFP (0.08–0.225 s; Figure 3B). Neural synchronization was larger for
386 young compared to aged rats ($p = 2.66 \times 10^{-4}$, $r_e = 0.234$, $df = 237$). These results indicate that the synaptic
387 inputs to the inferior colliculus neurons in response to a speech-like sound decrease in amplitude and
388 synchrony with age.

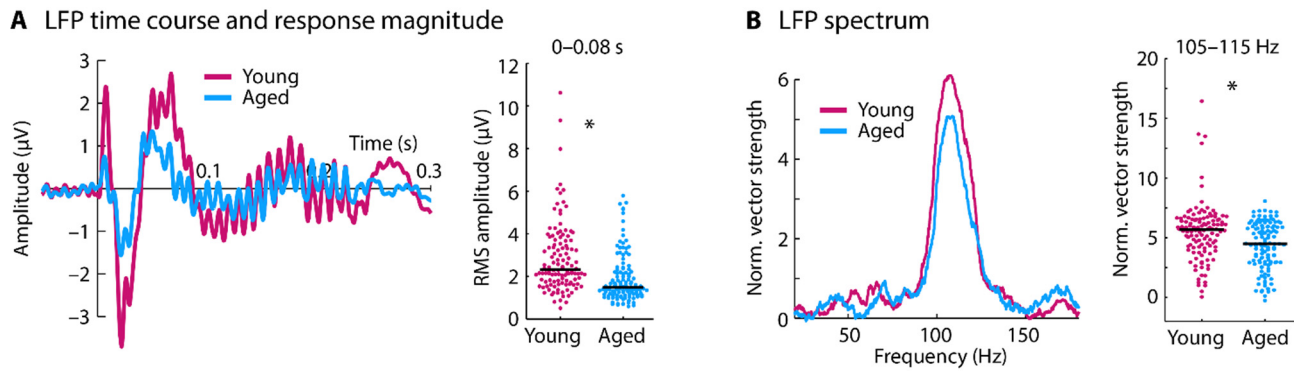


Figure 3: Time course and spectrum for local field potentials. A: Time course for each age group (left) and the root mean square (RMS) amplitude for the 0–0.08 s time window (right). **B:** Spectrum of normalized vector strength (left) and the mean vector strength for the 105–115 Hz frequency window (right). In panel A and B, each dot reflects the normalized vector strength of an individual unit. The black horizontal line reflects the median across units. * $p < 0.05$

389 ***Synchronization of multi-unit activity with the speech envelope are increased with age***

390 In order to investigate the consequences of the age-related decrease in synaptic inputs (indicated by
391 the LFPs) on the neural output of inferior colliculus neurons, multi-unit spiking activity was used as a
392 proxy for neural population or network responses in the inferior colliculus. Time courses for the multi-
393 unit activity (MUA) are shown in Figure 4. Spontaneous activity, quantified as the mean response in
394 the time window preceding sound onset (–0.05–0 s), was larger in aged compared to young rats ($p =$
395 2.91×10^{-10} , $r_e = 0.393$, $df = 237$; box plots in Figure 4A, left). Unlike the onset amplitudes of the LFPs (for
396 which responses were reduced for aged animals), there was no difference in MUA neuronal responses
397 to the sound onset (amplitude in the 0–0.08 s time window) between age groups ($p = 0.894$, $r_e =$
398 0.009 , $df = 237$; Figure 4A, middle and right).

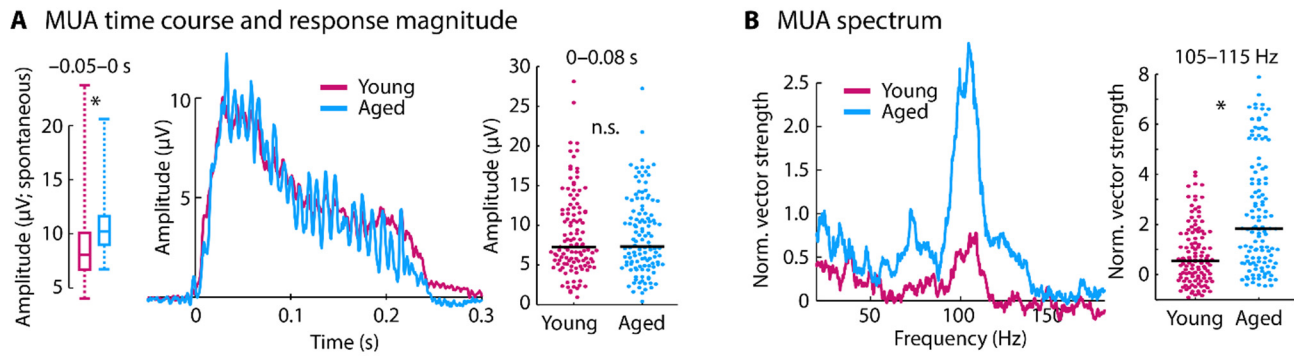


Figure 4: Time course and spectrum for multi-unit activity. **A:** Left: The box plots show the amplitude of the pre-stimulus onset time window ($-0.05-0$ s; i.e., spontaneous activity). Pre-stimulus onset activity was larger in aged compared to young animals ($p < 0.05$). Middle: Time course for each age group (data are baseline corrected, i.e., the mean response in the $-0.05-0$ s time window was subtracted from the amplitude at each time point). Right: Mean amplitude for the $0-0.08$ s time window. **B:** Spectrum of normalized vector strength (left) and the mean vector strength for the $105-115$ Hz frequency window (right). In panel A and B, each dot reflects the normalized vector strength of an individual unit. The black horizontal line is the median across units. * $p < 0.05$

399 Synchronization of MUA with the envelope of the sound was quantified using normalized vector
400 strength (Figure 4B). At the stimulation frequency (mean across the $105-115$ Hz frequency window),
401 neural synchronization was larger for aged compared to young rats ($p = 4.79 \times 10^{-9}$, $r_e = 0.367$, $df = 237$).
402 Taken together, the LFP and MUA results suggest a relative increase in neural response and an
403 increase in synchronization from a neuron's input to the neural population spiking output for aged
404 compared to young animals.

405 ***Synchronization of single-unit activity with the speech envelope are similar between young and***
406 ***aged animals***

407 Neuronal activity from well isolated neurons (single-unit activity) was analyzed in order to investigate
408 whether individual neurons in the aged inferior colliculus also show a relative enhancement of onset-
409 evoked activity and synchronization to the envelope.

410 Peri-stimulus time histograms for single-unit activity (SUA) are shown in Figure 5. Spontaneous
411 firing rates (i.e., in the $-0.05-0$ s time window) did not differ between age groups ($p = 0.831$, $r_e = 0.$
412 015 , $df = 210$). Firing rates to the sound onset ($0-0.08$ s) were larger for young compared to aged
413 animals ($p = 1.02e^{-4}$, $r_e = 0.268$, $df = 210$; Figure 5A). Neural synchronization to the envelope (F0) of the
414 sound measured using normalized vector strength showed no effect of age (mean across the 105–
415 115 Hz frequency window; $p = 0.703$, $r_e = 0.026$, $df = 210$; Figure 5B). Given the reduced LFP
416 synchronization, these results suggest an age-related increase in neural synchronization in single unit
417 activity (a neuron's output) relative to the LFP (synaptic input), albeit to a lesser degree than for multi-
418 unit activity.

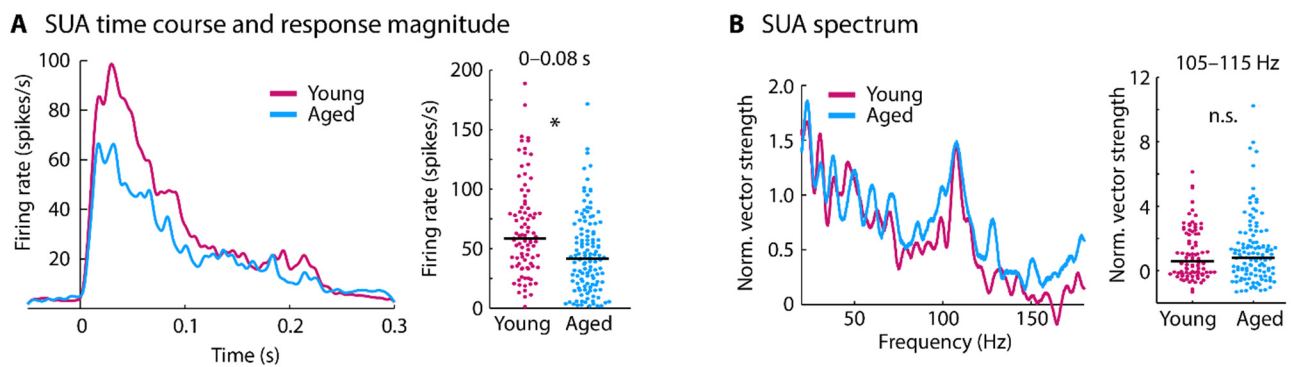


Figure 5: Time course and spectrum for single-unit activity. **A:** Peri-stimulus time histogram for each age group (left) and mean firing rate for the 0–0.08 s time window (right). **B:** Spectrum of normalized vector strength (left) and the mean vector strength for the 105–115 Hz frequency window (right). In panel A and B, each dot reflects the normalized vector strength of an individual unit. The black horizontal line is the median across units. * $p < 0.05$

419 ***Neural responses to a natural stimulus also show enhanced envelope sensitivity***

420 In order to examine whether the observed effects using the noise carrier also translate to real speech,
421 we additionally recorded neural activity in response to the original /ba/ speech sound for a subset of
422 units. Neurons responsive to this stimulus were found in lesser numbers due to the differences in the
423 frequency sensitivity of the rat's hearing range. Local field potentials and multi-unit activity was

424 recorded for 52 units in young animals and 20 units in aged animals. Single-unit activity was available
425 for 33 units in young animals and 20 units in aged animals.

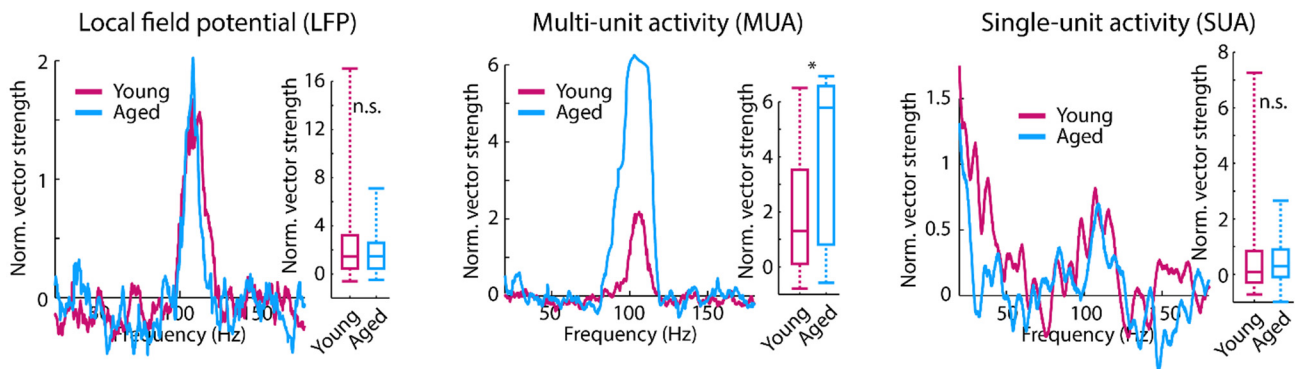


Figure 6: Spectrum of normalized vector strength for LFPs, MUA, and SUA in response to a speech sound. Box plots show the mean normalized vector strength for the 105–115 Hz frequency window. * $p < 0.05$, n.s. – not significant

426 The spectrum of normalized vector strength was calculated for LFPs, MUA, and SUA. The results
427 are displayed in Figure 6 and approximately mirror the results reported for the noise carrier. Effects
428 of aging on neural synchronization to the stimulus envelope were assessed by comparing the mean
429 normalized vector strength in the 105–115 Hz frequency window between age groups. For LFPs,
430 there was no difference in neural synchronization between age groups ($p = 0.730$, $r_e = 0.042$, $df = 70$).
431 An age-related increase in synchronization with the sound's envelope was observed for the MUA (p
432 $= 9.78 \times 10^{-3}$, $r_e = 0.303$, $df = 70$). For SUA, there was no effect of age for neural synchronization to the
433 envelope of the stimulus ($p = 0.345$, $r_e = 0.132$, $df = 51$).

434

Discussion

435 In the current study, we used a systems level (scalp recordings) and a micro-circuit level (LFPs and
436 unit activity) approach to investigate the age-related changes in neural sensitivity to temporal
437 regularity in a speech-like sound. Scalp-recorded potentials indicate that aging leads to a relative

438 increase in neural synchronization to the periodicity envelope along the ascending auditory pathway.
439 The underlying cellular changes in the midbrain were examined by recording neural activity from
440 neurons in the inferior colliculus in response to the speech-like sound. We used the local field
441 potential as a proxy for a neuron's or neural population's synaptic inputs, and multi-unit and single-
442 unit activity as a measure of spiking output. LFP amplitudes to the sound onset and LFP neural
443 synchronization to the temporal regularity of the envelope were smaller in aged compared to young
444 rats. In contrast, multi-unit activity and, to a lesser degree, single unit activity showed an aged-related
445 relative increase in synchronization to the periodicity envelope. Our results suggest that aging is
446 associated with altered sensitivity to sounds and a sound's temporal regularities, and that these
447 effects may be due to altered gain in neural network activity in the aged auditory midbrain.

448 ***Scalp-evoked potentials point to a decrease in brainstem responses and an increase in inferior***
449 ***colliculus responses***

450 Auditory brainstem responses (ABRs) and neural synchronization (i.e., EFRs) have been used to study
451 age-related changes in neural activity to speech and other complex sounds in humans (Stamper and
452 Johnson, 2015, Clinard and Tremblay, 2013, Anderson et al., 2012). The ability to obtain these
453 responses non-invasively makes them an ideal bridge between human studies and studies in animal
454 models, for which the underlying pathophysiology can additionally be studied at the micro-circuit
455 level using more invasive techniques (Zhong et al., 2014, Shaheen et al., 2015).

456 Consistent with previous studies (Fernandez et al., 2015, Sergeyenko et al., 2013,
457 Parthasarathy et al., 2014), we observed an age-related decrease in the wave 1 amplitude of the ABR
458 to clicks at suprathreshold sound levels (Figure 2A). The wave 1 of the ABR at suprathreshold sound
459 levels is a physiological indicator for the degree of cochlear synaptopathy, that is, the loss of the

460 synapses between inner hair cells and auditory nerve fibers (Kujawa and Liberman, 2009, Konrad-
461 Martin et al., 2012). The reduction of wave 1 in aged compared to young rats thus suggests the
462 presence of cochlear synaptopathy in the aged population used in the current study.

463 The sensitivity of the scalp-recorded EFRs to regular temporal structure in a speech-like sound
464 was investigated using measures of neural synchronization. We observed reduced synchronization
465 to the envelope and fine structure information for activity likely originating in the auditory nerve and
466 cochlear nucleus (Figure 2, left). Signals likely originating from rostral generators, including the
467 inferior colliculus, showed an age-related increase in neural synchronization to the envelope of the
468 speech-like sound (Figure 2B, C). These results suggest an age-related transformation in the neural
469 representation of envelope cues in speech along the ascending auditory pathway, which we
470 investigated further using more invasive extracellular electrophysiological methods.

471 ***Aging increases network level activity of inferior colliculus neurons relative to their synaptic inputs***

472 In order to study the contributions of the auditory midbrain to the changes seen in the scalp-recorded
473 responses, we simultaneously recorded LFPs and unit responses from the same site in response to
474 sound. LFPs are thought to be largely the aggregate pre-synaptic activity at the dendrites and the
475 soma, and hence a proxy for the inputs to the neuron or neuronal region (Buzsaki et al., 2012,
476 Gourevitch and Edeline, 2011, Logothetis and Wandell, 2004, Logothetis et al., 2001). By comparing
477 these LFPs to the spiking output, the transformation of these sound representations in the inferior
478 colliculus can be investigated (Herrmann et al., 2017).

479 In the current study, LFPs to the sound onset and neural synchronization to the sound's envelope
480 were decreased for aged compared to young rats (Figure 3), suggesting that inputs to the inferior
481 colliculus neurons are degraded. In contrast, multi-unit spiking activity in the inferior colliculus –
482 reflecting population or network output – revealed no age difference in the onset response and age-

483 related increase in synchronization to the sound's envelope (Figure 4). This relative enhancement
484 seen at the population level (MUA) was also present, albeit to a lesser degree, at the level of the single
485 neurons (SUA, Figure 5). These results suggest that the inferior colliculus neurons selectively increase
486 their neuronal activity to the envelope of a speech-like sound in aged animals, despite the reduced
487 synaptic inputs to these neurons.

488 Previous work suggested that midbrain neurons responding to simple stimuli like tones and
489 noise bursts show remarkably subtle changes with age (Willott et al., 1988a, Willott et al., 1988b). This
490 is despite the extensive degradation of the peripheral auditory system, such as the loss of outer hair
491 cells (Chen et al., 2009, Spongr et al., 1997), changes in endocochlear potential (Ohlemiller et al., 2006),
492 and the loss of cochlear synapses (Sergeyenko et al., 2013) and spiral ganglion neurons in the auditory
493 nerve (Bao and Ohlemiller, 2010). Even when studies using single-unit recordings do find age-related
494 changes in temporal processing (Palombi et al., 2001, Walton et al., 2002), it is unclear whether these
495 changes are inherited from previous stages of auditory processing, or generated in the nucleus being
496 studied. Our approach in this study shows that the enhancements seen in the spiking output of the
497 inferior colliculus neurons, in particular at the population and network level, may explain some of this
498 dichotomy in peripheral versus central responses with age.

499 ***Potential mechanisms underlying age-related changes in sensitivity to temporal regularity in***
500 ***sounds***

501 Acute insults (e.g., ototoxic drugs or mechanical deafening) to the auditory system damages the
502 auditory periphery and triggers homeostatic changes in the auditory pathway (Kotak et al., 2005,
503 Chambers et al., 2016). The most drastic change reported is a loss of inhibitory circuits and function
504 (Resnik and Polley, 2017, Caspary et al., 2013, Richardson et al., 2013, Ling et al., 2005), which, in turn,

505 increases neuronal activity in the central auditory structures (Chambers et al., 2016). The current data
506 in combination with recent evidence suggests that central auditory systems undergo similar gain
507 increases when the peripheral insult is gradual as is the case for aging (Lai et al., 2017, Parthasarathy
508 et al., 2014, Presacco et al., 2016).

509 The increase in neuronal activity due to a loss of inhibition is typically accompanied by a
510 reduction in the precision of neural coding. Inferior colliculus neurons change their tuning curves to
511 become less selective with age (Leong et al., 2011, Rabang et al., 2012). In addition, sensitivity to
512 temporal regularities in simple stimuli increases for slow amplitude modulations but decreases for
513 fast amplitude modulations in aged animals (Walton et al., 2002, Herrmann et al., 2017). In the current
514 study, inferior colliculus neurons in aged animals showed an increase in the spontaneous firing rate
515 (Figure 4A), which suggests inhibition was reduced in the aged midbrain. Furthermore, despite
516 reduced synaptic inputs to inferior colliculus neurons (as indexed by our LFP recordings), neuronal
517 firing of populations of inferior colliculus neurons was overly synchronized with the envelope of a
518 speech-like sound in aged compared to young animals (Figures 3 and 4). Our data thus suggest that
519 temporal response precision is altered in the aged midbrain due to hypersensitivity in networks of
520 neurons.

521 Increased gain in the auditory system may lead to better detection of weak signals in neural
522 circuits, and may, in turn, support hearing in quiet environments. However, such an enhancement
523 may come at the cost of poor discrimination between stimuli (Guo et al., 2017). Evidence from human
524 psychophysics supports this hypothesis; discrimination between fundamental frequency in speech is
525 reduced for older adults with clinically normal audiograms (Vongpoisal and Pichora-Fuller, 2007).
526 Hence, a neural gain increase in aging may improve detection of temporal regularity in sounds when

Envelope coding deficits with age in the IC

27

527 sounds occur in quiet, but may impair discrimination of temporal regularities in the presence of
528 background sound.

529

Conclusions

530 We investigated how aging affects neural sensitivity to temporal regularity in a speech-like sound.
531 Systems level recordings (i.e., at the scalp) were combined with microcircuit recordings (i.e., LFPs and
532 unit activity recorded extracellularly) in young and aged rats. We show that aging is associated with
533 increased neural activity along the ascending auditory pathway, which alters the sensitivity of
534 midbrain (i.e., inferior colliculus) neurons to temporally regular structure in sounds. Specifically,
535 synchronization to the periodicity envelope in speech (at the fundamental frequency) was enhanced
536 for spiking activity of populations of inferior colliculus neurons in aged rats, despite the neuron's
537 reduced synaptic input. The data suggest that temporal response precision is altered in the aged
538 midbrain due to hypersensitivity in networks of neurons.

539

Acknowledgements

540 This study was supported by NIDCD DC-011580 to ELB.

541

542

References

- 543 Allen, P. D. and Eddins, D. A. (2010) Presbycusis phenotypes form a heterogeneous continuum when
544 ordered by degree and configuration of hearing loss. *Hear Res* 264(1-2):10-20.
- 545 Anderson, S., Parbery-Clark, A., White-Schwoch, T. and Kraus, N. (2012) Aging Affects Neural Precision
546 of Speech Encoding. *J Neurosci* 32(41):14156-64.
- 547 Anderson, S., Parbery-Clark, A., Yi, H.-G. and Kraus, N. (2011) A Neural Basis of Speech-in-Noise
548 Perception in Older Adults. *Ear Hear* 32(6): 750-757.
- 549 Bao, J. X. and Ohlemiller, K. K. (2010) Age-related loss of spiral ganglion neurons. *Hear Res* 264(1-2):
550 93-97.
- 551 Bregman, A. S. (1990) *Auditory Scene Analysis; The Perceptual Organization of Sound*. Cambridge,
552 MA: MIT Press.
- 553 Buzsaki, G., Anastassiou, C. A. and Koch, C. (2012) The origin of extracellular fields and currents - EEG,
554 ECoG, LFP and spikes. *Nat Rev Neurosci* 13(6): 407-420.
- 555 Caspary, D. M., Hughes, L. F. and Ling, L. L. (2013) Age-related GABA(A) receptor changes in rat
556 auditory cortex. *Neurobiol Aging*. 34(5): 1486-1496.
- 557 Caspary, D. M., Ling, L., Turner, J. G. and Hughes, L. F. (2008) Inhibitory neurotransmission, plasticity
558 and aging in the mammalian central auditory system. *J Exp Biol*. 211(11): 1781-1791.
- 559 Chambers, A. R., Resnik, J., Yuan, Y. S., Whitton, J. P., Edge, A. S., Liberman, M. C. and Polley, D. B. (2016)
560 Central Gain Restores Auditory Processing following Near-Complete Cochlear Denervation.
561 *Neuron* 89(4): 867-879.
- 562 Chen, G. D., Li, M. N., Tanaka, C., Bielefeld, E. C., Hu, B. H., Kermany, M. H., Salvi, R. and Henderson, D.
563 (2009) Aging outer hair cells (OHCs) in the Fischer 344 rat cochlea: Function and morphology.
564 *Hear Res* 248(1-2): 39-47.
- 565 Clinard, C. G. and Tremblay, K. L. (2013) Aging Degrades the Neural Encoding of Simple and Complex
566 Sounds in the Human Brainstem. *J Am Acad Audiol* 24(7): 590-599.
- 567 Dayan, P. and Abbott, L. F. (2001) *Theoretical neuroscience: computational and mathematical*
568 *modeling of neural systems*. Cambridge, MA, USA: MIT Press.
- 569 Drummond, G. B. (2009) Reporting ethical matters in *The Journal of Physiology*: standards and advice.
570 *J Physiol*. 587: 713-719.
- 571 Dubno, J. R., Eckert, M. A., Lee, F. S., Matthews, L. J. and Schmiedt, R. A. (2013) Classifying Human
572 Audiometric Phenotypes of Age-Related Hearing Loss from Animal Models. *J Assoc Res*
573 *Otolaryngol*. 14(5): 687-701.
- 574 Fernandez, K. A., Jeffers, P. W. C., Lall, K., Liberman, M. C. and Kujawa, S. G. (2015) Aging after Noise
575 Exposure: Acceleration of Cochlear Synaptopathy in "Recovered" Ears. *J Neurosci* 35(19): 7509-
576 7520.
- 577 Frisina, D. R. and Frisina, R. D. (1997) Speech recognition in noise and presbycusis: Relations to
578 possible neural mechanisms. *Hear Res* 106(1-2): 95-104.
- 579 Fullgrabe, C., Moore, B. C. J. and Stone, M. A. (2015) Age-group differences in speech identification
580 despite matched audiometrically normal hearing: contributions from auditory temporal
581 processing and cognition. *Front Aging Neurosci* 6:347.
- 582 Gordon-Salant, S. and Fitzgibbons, P. J. (2001) Sources of age-related recognition difficulty for time-
583 compressed speech. *J Speech Lang Hear Res*. 44(4): 709-719.
- 584 Gourevitch, B. and Edeline, J. M. (2011) Age-related changes in the guinea pig auditory cortex:
585 relationship with brainstem changes and comparison with tone-induced hearing loss. *Eur J*
586 *Neurosci*. 34(12): 1953-1965.

- 587 Guo, W., Clause, A. R., Barth-Maron, A. and Polley, D. B. (2017) A Corticothalamic Circuit for Dynamic
588 Switching between Feature Detection and Discrimination. *Neuron*, 95(1): 180-194.
- 589 Herrmann, B., Parthasarathy, A. and Bartlett, E. L. (2017) Ageing affects dual encoding of periodicity
590 and envelope shape in rat inferior colliculus neurons. *Eur J Neurosci* 45(2): 299-311.
- 591 Herrmann, B., Parthasarathy, A., Han, E. X., Obleser, J. and Bartlett, E. L. (2015) Sensitivity of rat inferior
592 colliculus neurons to frequency distributions. *J Neurophysiol*. 114: 2941-2954.
- 593 Hughes, L. F., Turner, J. G., Parrish, J. L. and Caspary, D. M. (2010) Processing of broadband stimuli
594 across A1 layers in young and aged rats. *Hear Res*. 264(1-2): 79-85.
- 595 Konrad-Martin, D., Dille, M. F., McMillan, G., Griest, S., McDermott, D., Fausti, S. A. and Austin, D. F.
596 (2012) Age-Related Changes in the Auditory Brainstem Response. *J Am Acad Audiol*. 23(1): 18-
597 35.
- 598 Kotak, V. C., Fujisawa, S., Lee, F. A., Karthikeyan, O., Aoki, C. and Sanes, D. H. (2005) Hearing loss raises
599 excitability in the auditory cortex. *J Neurosci*. 25(15): 3908-3918.
- 600 Kujawa, S. G. and Liberman, M. C. (2009) Adding Insult to Injury: Cochlear Nerve Degeneration after
601 "Temporary" Noise-Induced Hearing Loss *J Neurosci*. 29(45): 14077-14085.
- 602 Lachaux, J.-P., Rodriguez, E., Martinerie, J. and Varela, F. J. (1999) Measuring Phase Synchrony in Brain
603 Signals. *Hum Brain Mapp* 8: 194-208.
- 604 Lai, J., Sommer, A. L. and Bartlett, E. L. (2017) Age-related changes in envelope-following responses at
605 equalized peripheral or central activation. *Neurobiol Aging*. 58: 191-200.
- 606 Lakatos, P., Musacchia, G., O'Connell, M. N., Falchier, A. Y., Javitt, D. C. and Schroeder, C. E. (2013) The
607 Spectrotemporal Filter Mechanism of Auditory Selective Attention. *Neuron*, 77(4): 750-761.
- 608 Lakatos, P., Shah, A. S., Knuth, K. H., Ulbert, I., Karmos, G. and Schroeder, C. E. (2005) An oscillatory
609 hierarchy controlling neuronal excitability and stimulus processing in the auditory cortex. *J*
610 *Neurophysiol* 94(3): 1904-1911.
- 611 Leong, U. C., Barsz, K., Allen, P. D. and Walton, J. P. (2011) Neural correlates of age-related declines in
612 frequency selectivity in the auditory midbrain. *Neurobiol Aging*, 32(1): 168-178.
- 613 Ling, L. L., Hughes, L. F. and Caspary, D. M. (2005) Age-related loss of the GABA synthetic enzyme
614 glutamic acid decarboxylase in rat primary auditory cortex. *Neuroscience*. 132(4): 1103-1113.
- 615 Logothetis, N. K., Pauls, J., Augath, M., Trinath, T. and Oeltermann, A. (2001) Neurophysiological
616 investigation of the basis of the fMRI signal. *Nature*, 412(6843): 150-157.
- 617 Logothetis, N. K. and Wandell, B. A. (2004) Interpreting the BOLD signal. *Annu Rev Physiol* 66: 735-
618 769.
- 619 Mohrle, D., Ni, K., Varakina, K., Bing, D., Lee, S. C., Zimmermann, U., Knipper, M. and Ruttiger, L. (2016)
620 Loss of auditory sensitivity from inner hair cell synaptopathy can be centrally compensated in
621 the young but not old brain. *Neurobiol Aging*. 44: 173-184.
- 622 Ohlemiller, K. K., Lett, J. M. and Gagnon, P. M. (2006) Cellular correlates of age-related endocochlear
623 potential reduction in a mouse model. *Hear Res*. 220(1-2): 10-26.
- 624 Palombi, P. S., Backoff, P. M. and Caspary, D. M. (2001) Responses of young and aged rat inferior
625 colliculus neurons to sinusoidally amplitude modulated stimuli. *Hear Res* 153(1-2): 174-180.
- 626 Parthasarathy, A. and Bartlett, E. (2012) Two-channel recording of auditory-evoked potentials to
627 detect age-related deficits in temporal processing. *Hear Res* 289(1-2): 52:62.
- 628 Parthasarathy, A., Datta, J., Torres, J. A. L., Hopkins, C. and Bartlett, E. L. (2014) Age-Related Changes in
629 the Relationship Between Auditory Brainstem Responses and Envelope-Following Responses. *J*
630 *Assoc Res Otolaryngol*. 15(4): 649-661.

- 631 Parthasarathy, A., Lai, J. and Bartlett, E. L. (2016) Age-Related Changes in Processing Simultaneous
632 Amplitude Modulated Sounds Assessed Using Envelope Following Responses. *J Assoc Res*
633 *Otolaryngol* 17(2): 119-132.
- 634 Paxinos, G. and Watson, C. (2006) *The Rat Brain in Stereotaxic Coordinates*. Academic Press.
- 635 Pichora-Fuller, M. K. and Souza, P. E. Effects of aging on auditory processing of speech. Workshop on
636 Candidature for and Delivery of Audiological Services - Special Needs of Older People, Eriksholm,
637 Denmark, Nov: B C Decker Inc, S11-S16.
- 638 Presacco, A., Simon, J. Z. and Anderson, S. (2016) Evidence of degraded representation of speech in
639 noise, in the aging midbrain and cortex. *J Neurophysiol.* 116(5): 2346-2355.
- 640 Rabang, C. F., Parthasarathy, A., Venkataraman, Y., Fisher, Z. L., Gardner, S. M. and Bartlett, E. L. (2012)
641 A computational model of inferior colliculus responses to amplitude modulated sounds in young
642 and aged rats. *Front Neural Circuits* 6:77.
- 643 Resnik, J. and Polley, D. B. (2017) Fast-spiking GABA circuit dynamics in the auditory cortex predict
644 recovery of sensory processing following peripheral nerve damage. *Elife*, 6.
- 645 Richardson, B. D., Ling, L. L., Uteshev, V. V. and Caspary, D. M. (2013) Reduced GABA(A) Receptor-
646 Mediated Tonic Inhibition in Aged Rat Auditory Thalamus. *J Neurosci.* 33(3): 1218-27a.
- 647 Rosen, S. (1992) Temporal information in speech - acoustic, auditory and linguistic aspects. *Philos*
648 *Trans R Soc Lond B Biol Sci.* 336(1278): 367-373.
- 649 Rosenthal, R. and Rubin, D. B. (2003) reequivalent: A Simple Effect Size Indicator. *Psychol Methods*, 8:
650 492-496.
- 651 Ruggles, D., Bharadwaj, H. and Shinn-Cunningham, B. G. (2011) Normal hearing is not enough to
652 guarantee robust encoding of suprathreshold features important in everyday communication.
653 *Proc Natl Acad Sci U S A.* 108(37): 15516-15521.
- 654 Schatteman, T. A., Hughes, L. F. and Caspary, D. M. (2008) Aged-related loss of temporal processing:
655 Altered responses to amplitude modulated tones in rat dorsal cochlear nucleus. *Neuroscience*,
656 154(1): 329-337.
- 657 Sergeyenko, Y., Lall, K., Liberman, M. C. and Kujawa, S. G. (2013) Age-Related Cochlear Synaptopathy:
658 An Early-Onset Contributor to Auditory Functional Decline. *J Neurosci.* 33(34): 13686-13694.
- 659 Shaheen, L. A., Valero, M. D. and Liberman, M. C. (2015) Towards a Diagnosis of Cochlear Neuropathy
660 with Envelope Following Responses. *J Assoc Res Otolaryngol.* 16(6): 727-45
- 661 Spongr, V. P., Flood, D. G., Frisina, R. D. and Salvi, R. J. (1997) Quantitative measures of hair cell loss in
662 CBA and C57BL/6 mice throughout their life spans. *J Acoust Soc Am.* 101(6): 3546-3553.
- 663 Stamper, G. C. and Johnson, T. A. (2015) Auditory Function in Normal-Hearing, Noise-Exposed Human
664 Ears. *Ear Hear.* 36(2): 172-184.
- 665 Syka, J. (2010) The Fischer 344 rat as a model of presbycusis. *Hear Res.* 264: 70-78.
- 666 Takesian, A. E., Kotak V. C., Sanes D. H. (2009) Developmental Hearing loss disrupts synaptic inhibition:
667 implications for auditory processing. *Future Neurol.*, 4(3):331-349
- 668 Vongpoisal, T. and Pichora-Fuller, M. K. (2007) Effect of age on F-0 difference limen and concurrent
669 vowel identification. *J Speech Lang Hear Res.* 50(5): 1139-1156.
- 670 Walton, J. P. (2010) Timing is everything: Temporal processing deficits in the aged auditory brainstem.
671 *Hear Res.* 264(1-2): 63-69.
- 672 Walton, J. P., Frisina, R. D. and O'Neill, W. E. (1998) Age-related alteration in processing of temporal
673 sound features in the auditory midbrain of the CBA mouse. *J Neurosci.* 18(7): 2764-2776.
- 674 Walton, J. P., Simon, H. and Frisina, R. D. (2002) Age-related alterations in the neural coding of
675 envelope periodicities. *J Neurophysiol.* 88(2): 565-578.

- 676 Willott, J. F., Parham, K. and Hunter, K. P. (1988a) Response properties of inferior colliculus neurons in
677 middle-aged C57bl/6J mice with presbycusis. *Hear Res.* 37(1): 15-27.
- 678 Willott, J. F., Parham, K. and Hunter, K. P. (1988b) Response properties of inferior colliculus neurons in
679 young and very old CBa/J mice. *Hear Res.* 37(1): 1-14.
- 680 Wolff, M. J., Jochim, J., Akyürek, E. G. and Stokes, M. G. (2017) Dynamic hidden states underlying
681 working-memory-guided behavior. *Nat Neurosci.* 20: 864-871.
- 682 Zhong, Z. W., Henry, K. S. and Heinz, M. G. (2014) Sensorineural hearing loss amplifies neural coding
683 of envelope information in the central auditory system of chinchillas. *Hear Res.* 309: 55-62.
- 684
- 685